

siRNA-Mediated Inhibition of $\text{Na}^+\text{--K}^+\text{--}2\text{Cl}^-$ Cotransporter (NKCC1) and Regulatory Volume Increase in the Chondrocyte Cell Line C-20/A4

Ala Qusous · Corinne S. V. Geewan ·
Pamela Greenwell · Mark J. P. Kerrigan

Received: 21 March 2011 / Accepted: 17 July 2011 / Published online: 17 August 2011
© Springer Science+Business Media, LLC 2011

Abstract The $\text{Na}^+\text{--K}^+\text{--}2\text{Cl}^-$ cotransporter (NKCC1) is an essential membrane transporter and has been linked to the regulation of volume, matrix synthesis and bone growth in chondrocytes; the sole resident cell type of articular cartilage. Despite the integral nature of NKCC1, its regulation is currently poorly understood, and therefore here we describe a NKCC1 knockdown technique that will permit the easier study of this transporter. Small interfering RNA (siRNA), designed to knock down *NKCC1*, was transfected into the chondrocyte cell line C-20/A4 and the efficacy determined at the message, protein and functional levels. *NKCC1* expression was analyzed by reverse-transcriptase polymerase chain reaction, where *NKCC1* expression declined to $25.10 \pm 1.08\%$ after 12 h of transfection and did not show any rise in the following 36 h. The efficacy of the designed siRNA molecules was confirmed by both Western blot and immunocytochemistry. The effect of the knockdown on regulatory volume increase (RVI, a novel assay for NKCC1 function) was investigated by confocal laser scanning microscopy in response to a 43% hypertonic challenge, whereby control chondrocytes underwent a decrease in volume to $67.38 \pm 1.70\%$, followed by volume restoration to 82.17 ± 2.23 at 20 min ($t_{1/2} = 22.11 \pm 3.23$ min). Conversely, upon knockdown, chondrocytes exhibited a slower rate of RVI ($t_{1/2} = 43.26 \pm 5.64$ min), thus suggesting that NKCC1 plays an important and yet partial role in RVI in C-20/A4 chondrocytes. Together, these data

provide a robust protocol for the study of NKCC1 in chondrocytes and suggest a mechanism for C-20/A4 chondrocyte RVI.

Keywords Chondrocyte · RVI · siRNA · Confocal · NKCC · C-20/A4 · Volume · Cartilage

Introduction

Chondrocytes are responsible for the synthesis of the extracellular cartilage matrix (ECM) in response to their extracellular environment as well as signals derived through mechanotransduction (Guilak et al. 1999; Hopewell and Urban 2003; Yellowley et al. 1997). Cellular homeostasis and, in particular, cell volume are important regulators of metabolic function, whereby an increase in extracellular osmolality and a consequent decrease in cell volume has been shown to attenuate matrix synthesis (Urban et al. 1993; van der Windt et al. 2010). Interestingly, changes in chondrocyte cell volume beyond the passive properties as a consequence of the ECM have been reported in both osteoarthritic tissue and the growth plate (Bush and Hall 2005; Bush et al. 2010), yet currently the mechanism is not fully understood. Indeed, one of the earliest macroscopic changes associated with osteoarthritis (OA) is an increase in cartilage hydration (Grushko et al. 1989), and recent in situ confocal laser scanning microscopy (CLSM) images of chondrocytes within human OA tissue revealed the existence of a sub-population of chondrocytes with a volume greater than that predicted by passive swelling alone (Bush and Hall 2005). Recently, a model for an increase in chondrocyte cell volume has been suggested during bone growth, which has been shown to be dependent upon the $\text{Na}^+\text{--K}^+\text{--}2\text{Cl}^-$ cotransporter (NKCC1) whereby an increase in NKCC1 mRNA was

A. Qusous · C. S. V. Geewan · P. Greenwell
School of Life Sciences, University of Westminster,
115 New Cavendish Street, London W1W 6UW, UK

M. J. P. Kerrigan (✉)
School of Science, University of Greenwich,
Chatham Maritime ME4 4TB, UK
e-mail: M.J.P.Kerrigan@greenwich.ac.uk

reported, as well as inhibition of growth, using bumetanide (Bush et al. 2010), a sulfamoylbenzoic acid derivative loop diuretic (Xu et al. 1994), thus suggesting a role for transporter activity in increasing chondrocyte volume despite a stable extracellular osmolality.

The gene of *NKCC1* is encoded on chromosome 5q23.2 and expressed by virtually all cell types (Flatman 2002). The protein is 1,212 amino acids long and has a total size of 132 kDa consisting of 12 transmembrane domains, five of which are inhibited by bumetanide. NKCC1 channels perform ATP-independent secondary active transport whereby a sodium ion, a chloride ion, a potassium ion and another chloride ion are consecutively bound to NKCC1, thus causing a configurational change. The ions are subsequently released into the cytoplasm in the same order (Flatman 2002). During regulatory volume increase (RVI), a process that adjusts the intracellular milieu following a hypertonic challenge by initiating a net influx of ion and other osmolytes (Trujillo et al. 1999b), this movement of ions results in the associated movement of water and the concomitant restoration of volume back toward the “set-point.” A role for NKCC1 in RVI has been shown in numerous tissues including avian chondrocytes (Ong et al. 2010), red blood cells (Kristensen et al. 2008), human glioma cells (Ernest and Sontheimer 2007), skeletal muscle cells (Zhao et al. 2004), epithelial cells (Bildin et al. 2000; Lionetto et al. 2002) and astrocytes (Jayakumar et al. 2008). NKCC1 is activated by phosphorylation, which promotes its translocation to the plasma membrane (Gimenez and Forbush 2003), a process occurring in response to cell shrinkage (Di Ciano-Oliveira et al. 2003) and a rise in intracellular calcium (Lytle and Forbush 1992). Yet, despite current activities in cartilage research, the regulation of NKCC1 is poorly understood (Ong et al. 2010).

RNA interference (RNAi) is a novel molecular technique that is based on a natural antiviral mechanism that involves interruption of gene expression at the mRNA translation level (Wang and Metzlafl 2005). Short (~ 21 nt long) double stranded (ds) sequences of small interfering RNA (siRNA), employed in this technique, bind to complementary sequences on the messenger and recruit the RNA-induced silencing complex (RISC) to degrade the message (Elbashir et al. 2001). RNAi gained increasing interest in molecular medicine as a gene therapy technique for knocking down dominant mutated genes in hereditary diseases including retinitis pigmentosa (Kiang et al. 2005) and viral sequences in infections including AIDS (Cullen 2005). In chondrocytes, RNAi has been used to study the role of various proteins including SOX9 (Wenke et al. 2009) and p16 (Zhou et al. 2004). RNAi, like similar techniques of gene therapy, still faces several drawbacks: (1) designing a suitable vector, which protects siRNA from the action of nucleases and delivers high concentrations to

particular tissues; (2) unlike gene knockout, RNAi has a transient effect, which does not possess the potential to cure permanent or chronic diseases; and (3) siRNA can instigate a nonspecific cytokine response (Bridge et al. 2003).

Due to the complexities of working with chondrocytes in situ, here we have designed and validated a process for siRNA against *NKCC1* in the human chondrocytic cell line C-20/A4 as a first step to further investigate the role of NKCC1 in cartilage biology. As the capacity for chondrocyte RVI has previously been reported (Kerrigan et al. 2006), this was used as a novel assay to determine the success of the knockdown as well as an indirect measure of both viability and function. Data show that following the optimization of siRNA transfection, a stable transient siRNA-mediated knockdown of *NKCC1* was achieved as determined at the messenger and functional levels, the latter determined by inhibition of NKCC1-mediated RVI following a hypertonic challenge. This method permits the easy study of NKCC1 in cartilage biology, which is essential for understanding the tissue in both healthy and diseased (OA) states.

Materials and Methods

Biochemicals and Experimental Solutions

Calcein AM was obtained from Cambridge Biosciences (Cambridge, UK), and stock solutions (1 mM) were prepared in DMSO. Other biochemicals, except where stated otherwise, were obtained from Sigma-Aldrich (Poole, UK), and a stock solution was made in the appropriate medium. For C-20/A4 culture, Dulbecco's modified Eagle medium (DMEM; pH 7.4; 280 mOsm·kg H₂O⁻¹, hereafter abbreviated mOsm, subsequently termed “culture medium”) was used with the addition of penicillin (100 units ml⁻¹), streptomycin (50 mg ml⁻¹), 10% v/v fetal calf serum (FCS; GIBCO, Paisley, UK) and 2 mM L-glutamine. RVI experiments were performed using a serum-free HEPES-buffered DMEM, and when a hypertonic challenge was applied, 620 mOsm DMEM (prepared by addition of NaCl, subsequently termed “hypertonic medium”) was added at a 1:1 ratio, resulting in an increase in osmolality to 440 mOsm. Osmolality was measured using a VaproTM-(Wescor, Stoneham, MA) vapor pressure osmometer with all solutions prepared to ±5 mOsm. pH was adjusted using NaOH to 7.4 ± 0.02, and all experiments were performed at 37°C.

Cell Culture and Viability

C-20/A4 can be used as a model when primary or embryonic cartilage is unavailable for use (Finger et al.

2004). C-20/A4 chondrocytes were cultured using standard techniques at a seeding density of 1×10^4 cells/cm² and subcultured when needed. Briefly, culture media were removed and chondrocytes incubated in trypsin-EDTA at 37°C, 95:5% air:CO₂ for 2–5 min. The suspension was then diluted with DMEM and washed by centrifugation (8 min, 600×g) and resuspended in fresh DMEM, aliquoted onto 35-mm-diameter sterile plastic dishes under sterile conditions and used as required (usually within 30 min). Cell viability was measured by MTT assay, where 10% v/v 5 mg/ml MTT solution was added to the culture and chondrocytes were incubated for 3 h at 37°C prior to the removal of medium containing excess MTT, the dissolution of formazan crystals in DMSO and measurement of absorbance at 570 and 690 nm per the manufacturer's protocol.

siRNA Design and Knockdown Protocol

The Ambion siRNA target online tool was utilized to select anti-*NKCC1* sequences with a GC content of a maximum of 50%, 2 nt UU-3' overhangs and stretches of no more than four mononucleotide repeats. All potential siRNA sense sequences were rated according to guidelines established by others (Reynolds et al. 2004), and sequences scoring less than 6 were excluded from further basic local alignment search (BLAST). Additionally, the chosen custom-designed siRNA fulfilled most of the guidelines established by other research (Ui-Tei et al. 2004). Anti-*NKCC1* siRNA in annealed form (Table 1), “positive” (anti-GAPDH siRNA) and “negative” (5'-carboxyfluorescein [FAM] labeled “scrambled” siRNA) controls were purchased from Ambion (Warrington, UK). Chondrocytes were transfected in suspension using siRNA complexes prepared with HiPerfect transfection reagent (Qiagen, Crawley, West Sussex, UK) as described by the manufacturer's protocol. siRNA was dissolved in serum-free DMEM, mixed with transfection reagent and incubated at room temperature for 10 min prior to dropwise addition to culture. To determine the knockdown efficiency of

HiPerfect in C-20/A4, a range of concentrations (1, 5, 10 nM) of anti-GAPDH-positive control siRNA were mixed with 18 µl/ml HiPerfect and transfection was performed and assayed by MTT viability assay.

Primer Design, PCR and Gel Densitometry

Primers for this work were designed using the Southwestern Medical Centre and RCE Region VI Computational Biology Group online tool according to the default parameters and subsequently checked for specificity (Table 1). RNA was isolated using the RNeasy minikit (Qiagen) and reverse-transcribed using the ImPromII reverse transcription kit (Promega, Southampton, UK) according to the manufacturer's protocol. PCR experiments were performed using 1 µM of each of the primers in GoTaq (Promega) PCR master mix. DNA was denatured for 5 min at 95°C and then subjected to a three-step cycle for 1 min at 95°C (denaturation), 1 min at 58°C (annealing) and 1 min at 72°C, followed by a final extension at 72°C for 5 min. PCR products were visualized on 2% agarose gels stained with ethidium bromide, and images were acquired for further densitometric analysis. Scion Image (Scion Corporation, Frederick, MD) was used to measure the size of DNA bands, intensity of band emission and background emission of the gel per the software instructions available on the Web site of the National Institutes of Health, with modifications. The methodology was developed by analyzing gels loaded with known amounts of various DNA lengths (data not shown) whereby, briefly, the background was subtracted from the intensity of each band and then multiplied by the size of the band. All values obtained in experiments were calculated relative to those corresponding to mock-transfected control amplicons.

Loading of Fluorescent Dyes and Volume Measurement

For the measurement of cell volume, chondrocytes were seeded and incubated with calcein AM (5 µM) for 30 min prior to CLSM imaging as previously described (Kerrigan and Hall 2008; Qusous et al. 2006). Briefly, images were acquired using a Leica (Milton Keynes, UK) SP2 CLSM whereby calcein was excited using a 488-nm argon laser and the photometric data collected at a bandpass of 510–535 nm. Data were sampled at 512×512 pixels, and 3D z-stacks were acquired using a z-step of 1.0 µm and reassembled in Imaris 7.0 (Bitplane, Zurich, Switzerland) using a 60% threshold. Experiments were performed following a 48-h transfection using anti-*NKCC1* (knockdown) or scrambled siRNA (control). Z-stacks were acquired for baseline and subsequently at 1.5, 3, 5, 10 and 20 min post-hypertonic challenge; and changes in cell volume are

Table 1 Sequences of PCR primers and siRNA molecules

Target	Direction	Sequence
PCR primer sequences		
<i>NKCC</i>	Forward	5'-TCGTCTTTCTGGAGTGGAAGA
	Reverse	5'-ATTGGCTTGATCGATGGAC
<i>GAPDH</i>	Forward	5'-AGAACGGGAAGCTTGTCATC
	Reverse	5'-TGAGCTTGACAAAGTGGTCGT
siRNA		
<i>NKCC</i>	Antisense	5'-UAUCUGUUAUUCGCCAUGGUU
	Sense	5'-CCAUGGCGAAUAACAGAUUU

expressed as percentage change relative to baseline volume values.

Immunocytochemistry

The localization of NKCC1 in control and *NKCC1*-knockdown chondrocytes was investigated using anti-*NKCC1* T4 ascetic fluid (Flatman 2002). Briefly, chondrocytes were fixed in 3% formaldehyde for 30 min at 37°C, and excess formaldehyde was quenched using 50 mM NH₄Cl prior to membrane permeabilization in 0.1% Triton X-100 for 5 min. Chondrocytes were washed in PBS and blocked in 1% goat serum for 1 h at room temperatures prior to the addition of 20 µl/ml of T4 antibodies (University of Iowa, Iowa City, IA) and allowing for hybridization overnight at 4°C (Lytle et al. 1995; Vardi et al. 2000). The sample was then rinsed, incubated with FITC-conjugated goat anti-mouse secondary antibody and 1 µg/ml propidium iodide (PI) for 2 h in the dark (20°C) and subsequently imaged by CLSM. Images were acquired by exciting FITC with a 488-nm argon laser, with photometric data collected at a bandpass of 510–535 nm, and PI was excited using a 488-nm Argon laser with photometric data collected using a long-pass filter. Data were sampled at 1,024 × 1,024 pixels using ×4 averaging to reduce the signal-to-noise ratio. 3D z-stacks were acquired at 0.5 µm to increase the detail of the image. For visualization of the FAM-labeled siRNA, transfected chondrocytes were fixed and permeabilized as described and chondrocytes were counterstained using 1 µM Topro-3 (Invitrogen, Carlsbad, CA) for 45 min to visualize the nucleus and cell cytoplasm. Images were acquired by CLSM, whereby FAM-labeled siRNA molecules were excited with a 488-nm argon laser, with photometric data collected at a bandpass of 510–535 nm, and Topro-3 was excited with a 633-nm He–Ne laser, with photometric data collected at a bandpass of 650–700 nm. Data were sampled at 1,024 × 1,024 pixels using ×4 averaging to reduce the signal-to-noise ratio. 3D z-stacks were acquired using a z-step of 0.5 µm exported in TIFF format for subsequent analysis in Imaris 7.0.

SDS-PAGE and Western Blot

The expression of *NKCC1* protein was investigated by SDS-PAGE, whereby cell lysis of 3 × 10⁵ chondrocytes was carried out in 50 µl lysis buffer (20 mM Tris-HCl, 120 mM NaCl, 1% Triton X-100, 10% glycerol, 1 mM sodium pyrophosphate, 20 mM sodium fluoride, 1 mM sodium orthovanadate [pH 7.5] containing protease inhibitor) prior to boiling in 50 µl 2× SDS-PAGE sample buffer at 95°C for 5 min. Protein samples were subsequently assayed prior to loading at 100 µg/well on 5.7%/12.5% polyacrylamide gel and blotted using a semidry transfer

assembly with ImmobilonTM-P transfer membrane (Millipore, Croyley, Watford, UK) according to the manufacturer's instructions. Following the transfer, the membrane was washed, blocked and incubated in 10 ml of Tween Tris-buffered saline (TBS/T) containing 10 µl T4 antibody with gentle agitation overnight at 4°C. The membrane was subsequently washed and incubated in 10 ml of TBS/T containing 5 µl goat horseradish peroxidase (HRP) anti-mouse IgG at room temperature for 1 h. Upon hybridization, the membrane was washed and incubated in 10 ml 1:1 luminol:hydrogen peroxide solution (Millipore) and exposed to X-ray film for 30 s, which was subsequently developed.

Data Presentation

All data are expressed as mean and standard error of the mean (SEM), and statistical analyses were performed using GraphPad (La Jolla, CA) Prism 5.0c. Regression analyses to calculate the rate of RVI were performed using Microsoft UK (Reading, UK) Excel, where $r^2 > 0.90$ was nominated as a significant fit and $t_{1/2}$ was defined as half the time required for chondrocytes to recover 100% of the volume following hypertonic challenge. The means of experiments were compared using Student's unpaired *t*-tests, and a significant difference was accepted when $P < 0.05$ or $P < 0.001$, represented in the figures as * or **, respectively. The number of cells (*n*) per experimental group is also given when appropriate.

Results and Discussion

Transfection Efficiency

Prior to determining the effects of *NKCC1* knockdown on the capacity for RVI and thus confirming a functional inhibition, it was necessary to establish a suitable transfection protocol by ascertaining the ratio of siRNA concentration to HiPerfect transfection reagent required for optimal transfection. Previously, the HiPerfect transfection reagent has been used in human carcinoma and leukemia cell lines (Wang et al. 2010; Ye et al. 2011), as well as leporine primary corneal stromal cell culture (Zhao et al. 2008) with high transfection efficiency and low toxicity (Fischer et al. 2010). In order to determine the efficiency of the transfection, a range of concentrations of transfection reagent complexed with three different concentrations of anti-GAPDH siRNA were used and cell death was determined by MTT assay 12 h posttransfection per the manufacturer's protocol (Fig. 1). Upon transfection, there was a significant increase in cell death ($P < 0.001$) under all conditions with $9.68 \pm 0.78\%$, $21.99 \pm 0.85\%$ and

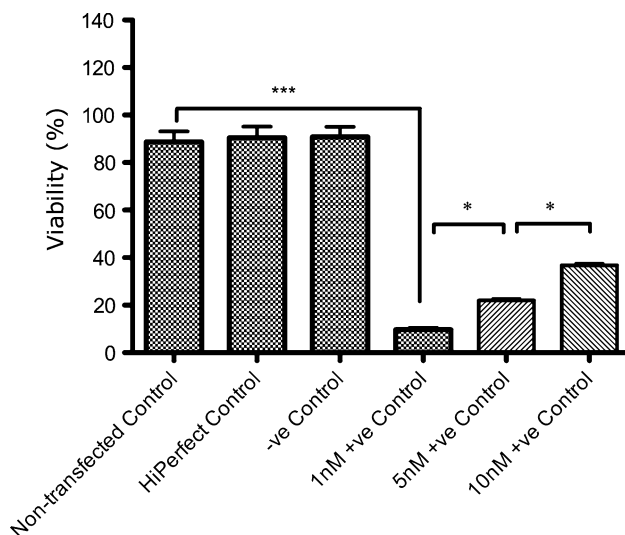


Fig. 1 Transfection optimization using anti-GAPDH siRNA and HiPerfect transfection reagent. The transfection efficiency of siRNA complexes prepared with HiPerfect was investigated in C-20/A4 chondrocytes using a range of concentrations of positive control anti-GAPDH siRNA (1, 5 and 10 nM) per the manufacturer's protocol. Successful knockdown resulted in the abolishment of GAPDH expression and, thus, cell death, as determined by MTT viability assay. There was a significant reduction in cell viability in response to transfection, indicating efficient knockdown using 18 μ l/ml HiPerfect, optimally observed in conjunction with 1 nM siRNA molecules

$36.77 \pm 0.94\%$ cell viability in 1-, 5- and 10-nM siRNA complexes, respectively. The effect of anti-GAPDH siRNA was deemed maximal at a ratio of 1 nM:18 μ l/ml of siRNA to HiPerfect transfection reagent (Qiagen), resulting in a transfection efficiency of $90.32 \pm 0.78\%$. This ratio was subsequently used for all other experiments.

Confocal Image of siRNA-Transfected Chondrocytes

Having determined a suitable transfection protocol, it was then necessary to ensure that the transfection did not influence the morphology of the C-20/A4 chondrocytes used in this study. Previous reports have shown that chondrocyte morphology is closely linked to cellular activity (Kerrigan and Hall 2008; Kerrigan et al. 2006) and that NKCC1 inhibition can result in a change in cell morphology (Chee et al. 2010). Following culture and passage, chondrocytes were transfected as previously described using a FAM-labeled control siRNA and observed by CLSM at 24 and 48 h posttransfection (Fig. 2). When visualized, FAM-labeled siRNA molecules (green) were clustered around the nucleus (blue, Topro3) with little staining toward the cell periphery. There was no discernable change in chondrocyte morphology, with the

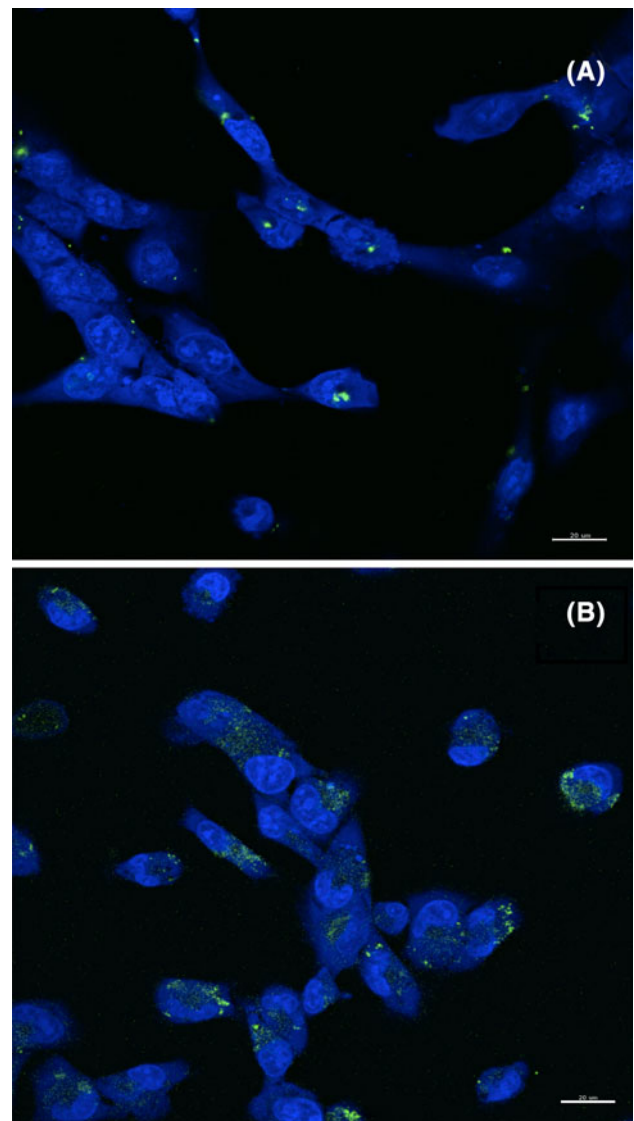


Fig. 2 Confocal image of FAM-labelled siRNA-transfected C-20/A4 chondrocytes. The localisation and uptake of FAM-labelled negative control siRNA (seen as specks) was investigated in response to transfection for 24 (a) and 48 hours (b) using CLSM. Chondrocytes were counterstained with Topro3 to observe perinuclear localisation of siRNA molecules against counterstained nuclei

cells maintaining their flattened appearance and attachment to the culture plastic both 24 and 48 h posttransfection.

siRNA Knockdown of NKCC1

As the transfection process did not influence chondrocyte morphology, and was thus deemed suitable, the next step of validating the protocol was to determine the efficacy of the siRNA knockdown of *NKCC1*. Therefore, chondrocytes were transfected as previously described, and a time course for the knockdown of *NKCC1* was studied by RT-PCR following siRNA transfection, whereby RNA extraction

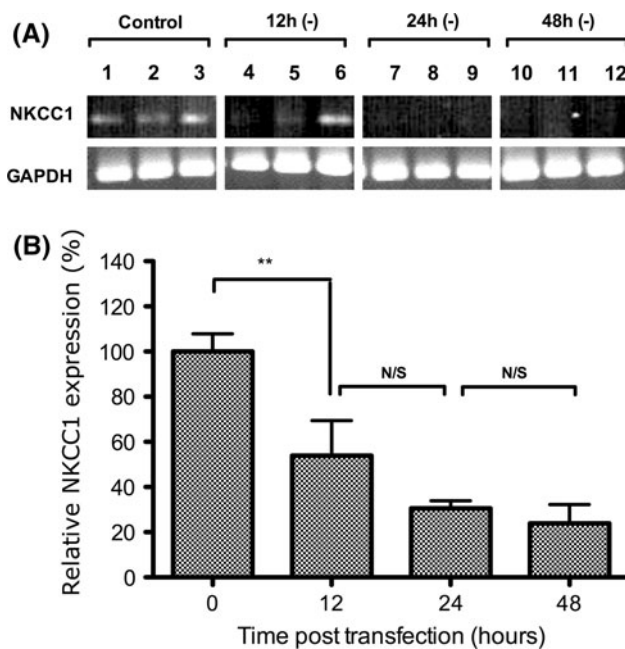


Fig. 3 Effects of custom-designed siRNA on NKCC1 expression. Chondrocytes were transfected with optimal concentrations of anti-NKCC1 siRNA (1 nM) and 18 μ l of HiPerfect transfection reagent and RNA was extracted after 12, 24 and 48 h posttransfection; reverse-transcribed; and amplified by PCR. NKCC1 knockdown was evident after 12 h of transfection and maintained for the remainder of the experiment (b). PCR gel images were used to quantify NKCC1 expression by densitometry (a). Data are shown as mean \pm SEM. $^{**}P < 0.001$

was performed at 0, 12, 24 and 48 h posttransfection. At 12 h posttransfection, there was a significant reduction in *NKCC1* RNA levels as determined by RT-PCR to $25.10 \pm 6.77\%$ compared to control mock-transfected chondrocytes (Fig. 3). There was no further change in the amount of *NKCC1* message upon further incubation with levels of $22.82 \pm 0.01\%$ and $24.25 \pm 0.01\%$ at 24 and 48 h posttransfection incubation periods (compared to control), respectively. Interestingly, it has been previously reported that *NKCC1* has a turnover rate of 83/s in endothelial cells (Kuang et al. 2001), yet despite this, these data demonstrated the efficiency of the custom-designed anti-*NKCC1* siRNA molecule, a successful transfection protocol and the sustained knockdown of the *NKCC1* message between 12 and at least 48 h posttransfection (Fig. 3), as previously reported in other mammalian cell lines (Elbashir et al. 2001).

While RT-PCR is a good tool for determining expression levels, it is conceivable that the NKCC1 knockdown could influence chondrocyte viability and, thus, not prove a suitable tool for its study. Therefore, chondrocyte viability was determined by MTT assay following transfection. When comparing cell viability upon NKCC1 knockdown groups and despite a reduction in cell division from a

Table 2 Summary of RVI properties in C-20/A4 chondrocytes upon *NKCC1* knockdown

	Mock-transfected control	Anti- <i>NKCC1</i> -transfected
Volume (μm^3)	$1,487.43 \pm 324.13$	$1,604.71 \pm 349.69$
Maximal recorded shrinkage (%)	69.32 ± 1.80	65.14 ± 2.00
Percentage recovery at $t = 20$ (%)	84.82 ± 2.07	74.54 ± 1.70
$t_{1/2}$ (min)	22.11 ± 3.23	43.26 ± 5.64
Viability (%)	90 ± 0.80	89.80 ± 1.41
Doubling time (days)	5.23 ± 0.26	13.94 ± 0.70

doubling time of 5.23 ± 0.26 days in non-transfected to 13.94 ± 0.70 days in anti-NKCC1 siRNA-transfected C-20/A4 chondrocytes (Table 2), there was no difference seen, suggesting that these cells remained suitable for subsequent studies while being transiently deficient in NKCC1. Similarly, upon NKCC1 inhibition using bumetanide, an arrest of the cell cycle was previously observed in airway smooth muscles without inducing cell death (Iwamoto et al. 2004). It must be noted, however, that siRNA transfection has been shown to intrinsically affect cellular growth (Ambion 2006); therefore, the reason for the inhibition of cell division upon *NKCC1* knockdown cannot be concluded.

Having determined that NKCC1 knockdown did not influence chondrocyte viability whilst significantly reducing NKCC1 RNA levels, it was then necessary to study the NKCC protein. Therefore, the localization of the NKCC1 protein was determined by immunocytochemistry and CLSM prior to transfection and repeated following siRNA-mediated knockdown. In control mock-transfected chondrocytes, the NKCC1 protein was localized along the plasma membrane (green) against a PI-counterstained nucleus (red) as previously reported in bovine corneal endothelial cells (Kuang et al. 2001); gerbile inner ear dark cells, strial marginal cells and kidney cells (Crouch et al. 1997); and human tracheobronchial smooth muscle (Iwamoto et al. 2003). Conversely, following anti-*NKCC1* knockdown for 48 h, it was not possible to detect any NKCC1, thus confirming the effect of mRNA knockdown on protein levels (Fig. 4a). To further confirm the effect of knockdown on NKCC1 content in total cell protein lysate, Western blot was performed as previously described. Upon knockdown there was a distinct reduction of the NKCC1 protein upon performing SDS-PAGE (Fig. 4b).

Traditionally, NKCC1 is studied using 86-rubidium (O'Donnell 1993) and inhibited using bumetanide, which additionally inhibits other members of the solute carrier family of membrane transporters, including the monocarboxylic acid transporter 7 (Price et al. 1998; Xu et al.

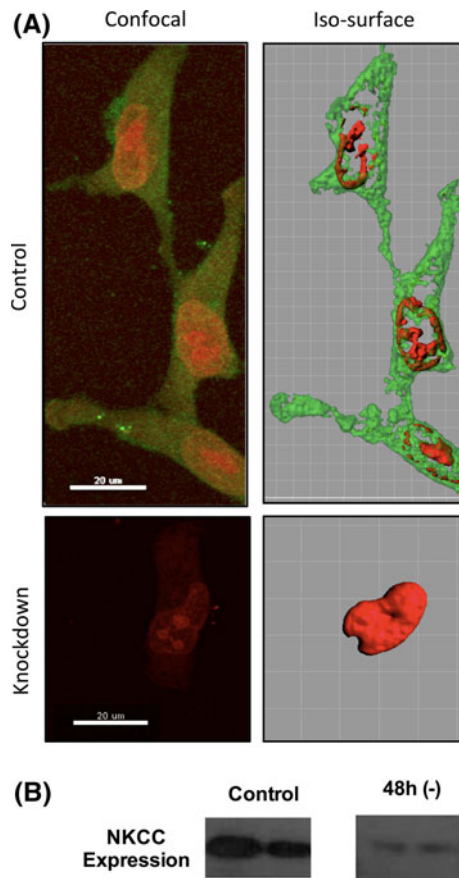


Fig. 4 The effect of anti-NKCC1 siRNA transfection on the protein level. Chondrocytes were transfected with anti-NKCC1 siRNA for 48 hours, fixed and visualised using T4 antibodies and secondary Alexa-488 antibodies (staining the plasma membrane) against background nuclear staining using propidium iodide. A reduction in the amount of NKCC1 protein was visible upon knockdown (a) and was further confirmed by western blot using T4 and HRP-secondary antibodies (b)

1994). Here, we report expression of *NKCC1* in the C-20/A4 chondrocytic cell line at both the mRNA and protein levels by RT-PCR and Western blot, respectively, and we have devised a molecular method of inhibiting NKCC1 activity by message knockdown. These data combined demonstrate the successful knockdown of NKCC1 at both the message and protein levels, while not influencing chondrocyte viability or morphology.

Capacity for RVI in Knockdown Chondrocytes

Having determined a successful protocol for knockdown of NKCC1, we then wanted to confirm this by using the capacity for RVI as a novel assay. The response of C-20/A4 chondrocytes to hypertonicity was investigated with and without knockdown of *NKCC1*. Previous reports have shown that inhibition of NKCC1 using bumetanide induced cell shrinkage in lens fiber cells and vascular smooth muscles (Anfinogenova et al. 2004; Chee et al.

2010), whereas there was no significant difference ($P > 0.05$) in the resting cell volume of mock (negative control siRNA) transfected and anti-*NKCC1*-transfected chondrocytes at 280 mOsm (determined at $1,487.43 \pm 324.13 \mu\text{m}^3$ and $1,604.71 \pm 349.69 \mu\text{m}^3$, respectively; Table 2). These values were significantly larger than those observed in freshly isolated bovine and human articular chondrocytes (Bush and Hall 2001, 2003) but are not different when compared to other chondrocytic cell lines including A13/BACii (Qusous et al. 2010).

The role of NKCC1 in C-20/A4 RVI was determined by studying changes in chondrocyte cell volume in response to a hypertonic challenge by CLSM in control and anti-*NKCC1* siRNA-transfected chondrocytes 48 h posttransfection. In all experimental conditions there was no significant difference in cell shrinkage ($P > 0.05$) (Fig. 5) whereby chondrocytes decreased in volume to $67.38 \pm 1.66\%$ and $65.26 \pm 1.86\%$ in mock and anti-*NKCC1*-transfected chondrocytes, respectively, as recorded at 1.5 min post-challenge. Mock-transfected chondrocytes then exhibited RVI with a $t_{1/2}$ of 22.11 ± 3.23 min and $82.17 \pm 2.23\%$ volume recovery within the 20-min experimental period. Conversely, in the presence of anti-*NKCC1* siRNA chondrocytes exhibited attenuated RVI with a reduction in $t_{1/2}$ to 43.26 ± 5.64 min and only $73.78 \pm 1.60\%$ volume recovered during the experimental period at 20 min. Together these data show that siRNA-mediated knockdown of NKCC1 inhibits the capacity for RVI, thus confirming the reduction in functional protein expression at 24 h post-transfection. Interestingly, these data were also found to be

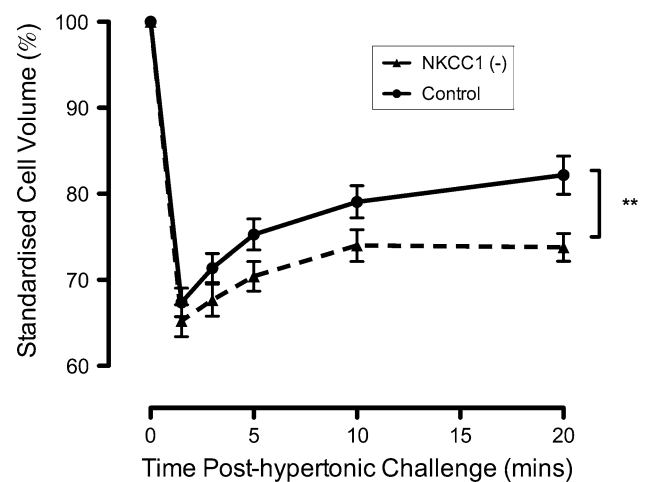


Fig. 5 Changes in volume in response to hyperosmotic challenge in control and knockdown chondrocytes. Chondrocytes were loaded with calcein AM and subjected to a 43% hyperosmotic challenge, and changes in cell volume were recorded using CLSM. The volume of the chondrocytes decreased and then sharply increased within 5 min. Conversely, upon NKCC1 knockdown, chondrocytes exhibited a slower rate of volume recovery. Data are shown as mean \pm SEM. Number of cells, $n = 86$. ** $P < 0.001$

similar to rates of RVI previously reported in avian chondrocytes (Ong et al. 2010) and strongly suggest that the mechanism for RVI in the chondrocytic cell line C-20/A4 is mediated, but not exclusively, by NKCC1.

It was previously observed that freshly isolated chondrocytes do not have the capacity for robust RVI whereas, upon 2D culture, RVI is evident and principally mediated by NKCC1 (Kerrigan et al. 2006). Here, we report that C-20/A4 chondrocytes have the capacity for NKCC1-dependent RVI at a slower rate compared to 2D cultured “responding” chondrocytes. Interestingly, C-20/A4 chondrocytes were found to possess a large cell volume ($>600 \mu\text{m}^3$; Table 2), similar to previous reports in fetal chondrocytes of the reserve zone (Melrose et al. 2008), hypertrophic chondrocytes (Bohme et al. 1995; DeLise et al. 2000) and chondrocytes from degenerate cartilage (Bush and Hall 2003, 2005). Furthermore, despite upregulation of NKCC1 having been previously reported in hypertrophic tissue (Bush et al. 2010), no change in NKCC1 expression was observed upon 2D culture of fetal human chondrocytes (Stokes et al. 2002) or tissue degeneration (Trujillo et al. 1999a). It is thus conceivable that a change in NKCC activity, possibly regulated by actin organization (Lionetto et al. 2002; Ong et al. 2010) via a cAMP-dependent pathway (D’Andrea et al. 1996; Gosmanov and Thomason 2003) or WNK phosphorylation (Kahle et al. 2010), may account for the RVI or an increased cell volume in chondrocytes.

Following siRNA knockdown, C-20/A4 chondrocytes still exhibited the capacity for robust volume regulation, most likely attributed to the activity of other membrane transporters including the epithelial sodium channel (ENaC), previously observed in arthritic chondrocytes (Trujillo et al. 1999a), or the Na^+/H^+ exchanger (Browning and Wilkins 2004).

Conclusion

Here, we have demonstrated the effective use of a highly specific molecular inhibitory tool (RNAi) to target *NKCC1* in chondrocytes at the message, protein and functional levels while not influencing chondrocyte viability or morphology. The use of this technology to functionally inhibit NKCC1 has been demonstrated by ablating the capacity for RVI, thus suggesting that this model is suitable for the additional study of this transporter. Currently, further work is still required to better understand the activation of NKCC1 in chondrocytes and its potential role in OA, and siRNA technology offers a suitable tool for this.

Acknowledgments The authors thank Dr. Ian Locke for donating C-20/A4 chondrocytes, Dr. Peter Flatman for the initial sample of T4

antibodies and Dr. Sanjiv Rughooputh for his assistance and feedback. This work was partly funded by the Wellcome Trust and made possible thanks to Mr. Aiman T. Qusous and Ms. Najda Goussous. T4 antibody (contribution of Lytle and Forbush III) was obtained from the Developmental Studies Hybridoma Bank developed under the auspices of the NICHD and maintained by The University of Iowa, Department of Biology (Iowa City, IA 52242).

References

- Ambion (2006) RNAi goes genomic: elucidating gene function with siRNA libraries. www.ambion.com/techlib/webcasts/siRNA0606.pdf
- Anfinogenova YJ, Baskakov MB, Kovalev IV, Kilin AA, Dulin NO, Orlov SN (2004) Cell-volume-dependent vascular smooth muscle contraction: role of Na^+ , K^+ , 2Cl^- cotransport, intracellular Cl^- and L-type Ca^{2+} channels. *Pflugers Arch* 449:42–55
- Bildin VN, Yang H, Crook RB, Fischbarg J, Reinach PS (2000) Adaptation by corneal epithelial cells to chronic hypertonic stress depends on upregulation of $\text{Na}:\text{K}:2\text{Cl}$ cotransporter gene and protein expression and ion transport activity. *J Membr Biol* 177:41–50
- Bohme K, Winterhalter KH, Bruckner P (1995) Terminal differentiation of chondrocytes in culture is a spontaneous process and is arrested by transforming growth factor-beta 2 and basic fibroblast growth factor in synergy. *Exp Cell Res* 216:191–198
- Bridge AJ, Pebernard S, Ducraux A, Nicoulaz AL, Iggo R (2003) Induction of an interferon response by RNAi vectors in mammalian cells. *Nat Genet* 34:263–264
- Browning JA, Wilkins RJ (2004) Mechanisms contributing to intracellular pH homeostasis in an immortalised human chondrocyte cell line. *Comp Biochem Physiol A Mol Integr Physiol* 137:409–418
- Bush PG, Hall AC (2001) The osmotic sensitivity of isolated and in situ bovine articular chondrocytes. *J Orthop Res* 19:768–778
- Bush PG, Hall AC (2003) The volume and morphology of chondrocytes within non-degenerate and degenerate human articular cartilage. *Osteoarthritis Cartilage* 11:242–251
- Bush PG, Hall AC (2005) Passive osmotic properties of in situ human articular chondrocytes within non-degenerate and degenerate cartilage. *J Cell Physiol* 204:309–319
- Bush PG, Pritchard M, Loqman MY, Damron TA, Hall AC (2010) A key role for membrane transporter NKCC1 in mediating chondrocyte volume increase in the mammalian growth plate. *J Bone Miner Res* 25:1594–1603
- Chee KN, Vorontsova I, Lim JC, Kistler J, Donaldson PJ (2010) Expression of the sodium potassium chloride cotransporter (NKCC1) and sodium chloride cotransporter (NCC) and their effects on rat lens transparency. *Mol Vis* 16:800–812
- Crouch JJ, Sakaguchi N, Lytle C, Schulte BA (1997) Immunohistochemical localization of the $\text{Na}-\text{K}-\text{Cl}$ co-transporter (NKCC1) in the gerbil inner ear. *J Histochem Cytochem* 45:773–778
- Cullen BR (2005) Does RNA interference have a future as a treatment for HIV-1 induced disease? *AIDS Rev* 7:22–25
- D’Andrea L, Lytle C, Matthews JB, Hofman P, Forbush B 3rd, Madara JL (1996) $\text{Na}:\text{K}:2\text{Cl}$ cotransporter (NKCC) of intestinal epithelial cells. Surface expression in response to cAMP. *J Biol Chem* 271:28969–28976
- DeLise AM, Fischer L, Tuan RS (2000) Cellular interactions and signaling in cartilage development. *Osteoarthritis Cartilage* 8:309–334
- Di Ciano-Oliveira C, Sirokmany G, Szaszi K, Arthur WT, Masszi A, Peterson M, Rotstein OD, Kapus A (2003) Hyperosmotic stress activates Rho: differential involvement in Rho kinase-dependent

- MLC phosphorylation and NKCC activation. *Am J Physiol Cell Physiol* 285:C555–C566
- Elbashir SM, Harborth J, Lendeckel W, Yalcin A, Weber K, Tuschl T (2001) Duplexes of 21-nucleotide RNAs mediate RNA interference in cultured mammalian cells. *Nature* 411:494–498
- Ernest NJ, Sontheimer H (2007) Extracellular glutamine is a critical modulator for regulatory volume increase in human glioma cells. *Brain Res* 1144:231–238
- Finger F, Schorle C, Soder S, Zien A, Goldring MB, Aigner T (2004) Phenotypic characterization of human chondrocyte cell line C-20/A4: a comparison between monolayer and alginate suspension culture. *Cells Tissues Organs* 178:65–77
- Fischer W, Calderon M, Schulz A, Andreou I, Weber M, Haag R (2010) Dendritic polyglycerols with oligoamine shells show low toxicity and high siRNA transfection efficiency in vitro. *Bioconjug Chem* 21:1744–1752
- Flatman PW (2002) Regulation of Na-K-2Cl cotransport by phosphorylation and protein–protein interactions. *Biochim Biophys Acta* 1566:140–151
- Gimenez I, Forbush B (2003) Short-term stimulation of the renal Na-K-Cl cotransporter (NKCC2) by vasopressin involves phosphorylation and membrane translocation of the protein. *J Biol Chem* 278:26946–26951
- Gosmanov AR, Thomason DB (2003) Regulation of $\text{Na}^+\text{-K}^+\text{-2Cl}^-$ cotransporter activity in rat skeletal muscle and intestinal epithelial cells. *Tsitologiya* 45:812–816
- Grushko G, Schneiderman R, Maroudas A (1989) Some biochemical and biophysical parameters for the study of the pathogenesis of osteo-arthritis—a comparison between the processes of aging and degeneration in human hip cartilage. *Connect Tissue Res* 19:149–176
- Guilak F, Jones WR, Ting-Beall HP, Lee GM (1999) The deformation behavior and mechanical properties of chondrocytes in articular cartilage. *Osteoarthritis Cartilage* 7:59–70
- Hopewell B, Urban JP (2003) Adaptation of articular chondrocytes to changes in osmolality. *Biorheology* 40:73–77
- Iwamoto LM, Nakamura KT, Wada RK (2003) Immunolocalization of a Na-K-2Cl cotransporter in human tracheobronchial smooth muscle. *J Appl Physiol* 94:1596–1601
- Iwamoto LM, Fujiwara N, Nakamura KT, Wada RK (2004) Na-K-2Cl cotransporter inhibition impairs human lung cellular proliferation. *Am J Physiol Lung Cell Mol Physiol* 287:L510–L514
- Jayakumar AR, Liu M, Moriyama M, Ramakrishnan R, Forbush B III, Reddy PV, Norenberg MD (2008) Na-K-Cl Cotransporter-1 in the mechanism of ammonia-induced astrocyte swelling. *J Biol Chem* 283:33874–33882
- Kahle KT, Rinehart J, Lifton RP (2010) Phosphoregulation of the Na-K-2Cl and K-Cl cotransporters by the WNK kinases. *Biochim Biophys Acta* 1802:1150–1158
- Kerrigan MJ, Hall AC (2008) Control of chondrocyte regulatory volume decrease (RVD) by $[\text{Ca}^{2+}]_i$ and cell shape. *Osteoarthritis Cartilage* 16:312–322
- Kerrigan MJ, Hook CS, Qusous A, Hall AC (2006) Regulatory volume increase (RVI) by in situ and isolated bovine articular chondrocytes. *J Cell Physiol* 209:481–492
- Kiang AS, Palfi A, Ader M, Kenna PF, Millington-Ward S, Clark G, Kennan A, O'Reilly M, Tam LC, Aherne A, McNally N, Humphries P, Farrar GJ (2005) Toward a gene therapy for dominant disease: validation of an RNA interference-based mutation-independent approach. *Mol Ther* 12:555–561
- Kristensen K, Berenbrink M, Koldkjaer P, Abe A, Wang T (2008) Minimal volume regulation after shrinkage of red blood cells from five species of reptiles. *Comp Biochem Physiol A Mol Integr Physiol* 150:46–51
- Kuang K, Li Y, Wen Q, Wang Z, Li J, Yang Y, Iserovich P, Reinach PS, Sparrow J, Diecke FP, Fischbarg J (2001) Corneal endothelial NKCC: molecular identification, location, and contribution to fluid transport. *Am J Physiol Cell Physiol* 280:C491–C499
- Lionetto MG, Pedersen SF, Hoffmann EK, Giordano ME, Schettino T (2002) Roles of the cytoskeleton and of protein phosphorylation events in the osmotic stress response in eel intestinal epithelium. *Cell Physiol Biochem* 12:163–178
- Lytle C, Forbush B 3rd (1992) The Na-K-Cl cotransport protein of shark rectal gland. II. Regulation by direct phosphorylation. *J Biol Chem* 267:25438–25443
- Lytle C, Xu JC, Biemesderfer D, Forbush B 3rd (1995) Distribution and diversity of Na-K-Cl cotransport proteins: a study with monoclonal antibodies. *Am J Physiol Cell Physiol* 269:C1496–C1505
- Melrose J, Smith SM, Smith MM, Little CB (2008) The use of Histochoice for histological examination of articular and growth plate cartilages, intervertebral disc and meniscus. *Biotech Histochem* 83:47–53
- O'Donnell ME (1993) Role of Na-K-Cl cotransport in vascular endothelial cell volume regulation. *Am J Physiol Cell Physiol* 264:C1316–C1326
- Ong SB, Shah D, Qusous A, Jarvis SM, Kerrigan MJ (2010) Stimulation of regulatory volume increase (RVI) in avian articular chondrocytes by gadolinium chloride. *Biochem Cell Biol* 88:505–512
- Price NT, Jackson VN, Halestrap AP (1998) Cloning and sequencing of four new mammalian monocarboxylate transporter (MCT) homologues confirms the existence of a transporter family with an ancient past. *Biochem J* 329(Pt 2):321–328
- Qusous A, Hook C, McRobb L, Kerrigan MJP (2006) siRNA mediated inhibition of regulatory volume increase (RVI) in the chondrocyte cell line C-20/A4. In: Orthopaedic Research Society (ORS) Transactions. ORS, Chicago, p 0291
- Qusous A, Kaneva M, Getting SJ, Kerrigan MJP (2010) A13/BACII, a novel bovine chondrocytic cell line with differentiation potential. Paper presented at the 2010 Combined Meeting of Orthopaedic Research Societies (CORS), Kyoto, October 16 (Sat.)–20 (Wed.), 2010.
- Reynolds A, Leake D, Boese Q, Scaringe S, Marshall WS, Khvorova A (2004) Rational siRNA design for RNA interference. *Nat Biotechnol* 22:326–330
- Stokes DG, Liu G, Coimbra IB, Piera-Velazquez S, Crowl RM, Jimenez SA (2002) Assessment of the gene expression profile of differentiated and dedifferentiated human fetal chondrocytes by microarray analysis. *Arthritis Rheum* 46:404–419
- Trujillo E, Alvarez de la Rosa D, Mobasheri A, Avila J, Gonzalez T, Martin-Vasallo P (1999a). Sodium transport systems in human chondrocytes. I. Morphological and functional expression of the $\text{Na}^+\text{-K}^+\text{-ATPase}$ alpha and beta subunit isoforms in healthy and arthritic chondrocytes. *Histol Histopathol* 14:1011–1022
- Trujillo E, Alvarez de la Rosa D, Mobasheri A, Gonzalez T, Canessa CM, Martin-Vasallo P (1999b) Sodium transport systems in human chondrocytes II. Expression of ENaC, $\text{Na}^+\text{-K}^+\text{-2Cl}^-$ cotransporter and $\text{Na}^+\text{-H}^+$ exchangers in healthy and arthritic chondrocytes. *Histol Histopathol* 14:1023–1031
- Ui-Tei K, Naito Y, Takahashi F, Haraguchi T, Ohki-Hamazaki H, Juni A, Ueda R, Saigo K (2004) Guidelines for the selection of highly effective siRNA sequences for mammalian and chick RNA interference. *Nucleic Acids Res* 32:936–948
- Urban JP, Hall AC, Gehl KA (1993) Regulation of matrix synthesis rates by the ionic and osmotic environment of articular chondrocytes. *J Cell Physiol* 154:262–270
- van der Windt AE, Haak E, Das RH, Kops N, Welting TJ, Caron MM, van Til NP, Verhaar JA, Weinans H, Jahr H (2010) Physiological tonicity improves human chondrogenic marker expression through nuclear factor of activated T-cells 5 in vitro. *Arthritis Res Ther* 12:R100

- Vardi N, Zhang LL, Payne JA, Sterling P (2000) Evidence that different cation chloride cotransporters in retinal neurons allow opposite responses to GABA. *J Neurosci* 20:7657–7663
- Wang MB, Metzlauff M (2005) RNA silencing and antiviral defense in plants. *Curr Opin Plant Biol* 8:216–222
- Wang TY, Feng SQ, Zhang ZX, Shi XD, Liu R, Liu ZQ (2010) Suppression of survivin gene in leukemia cells by small interfering RNA [in Chinese]. *Zhonghua Er Ke Za Zhi* 48:843–847
- Wenke AK, Grassel S, Moser M, Bosserhoff AK (2009) The cartilage-specific transcription factor Sox9 regulates AP-2epsilon expression in chondrocytes. *FEBS J* 276:2494–2504
- Xu JC, Lytle C, Zhu TT, Payne JA, Benz E Jr, Forbush B 3rd (1994) Molecular cloning and functional expression of the bumetanide-sensitive Na-K-Cl cotransporter. *Proc Natl Acad Sci USA* 91:2201–2205
- Ye D, Zhang HF, Zhu LY, Wang LW, Chen LX (2011) CIC-3 siRNA inhibits regulatory volume decrease in nasopharyngeal carcinoma cells [in Chinese]. *Nan Fang Yi Ke Da Xue Xue Bao* 31:216–220
- Yellowley CE, Jacobs CR, Li Z, Zhou Z, Donahue HJ (1997) Effects of fluid flow on intracellular calcium in bovine articular chondrocytes. *Am J Physiol Cell Physiol* 273:C30–C36
- Zhao H, Hyde R, Hundal HS (2004) Signalling mechanisms underlying the rapid and additive stimulation of NKCC activity by insulin and hypertonicity in rat L6 skeletal muscle cells. *J Physiol* 560:123–136
- Zhao GQ, Du ZD, Liang T, Liu JW, Zhang LN, Zhang ZH (2008) RNA interference inhibits expression of cyclooxygenase-2 and matrix metalloproteinase-2 in rabbit corneal stromal cells [in Chinese]. *Zhonghua Yan Ke Za Zhi* 44:831–838
- Zhou HW, Lou SQ, Zhang K (2004) Recovery of function in osteoarthritic chondrocytes induced by p16INK4a-specific siRNA in vitro. *Rheumatology (Oxford)* 43:555–568